JOURNAL OF CATALYSIS **166,** 272–283 (1997)
ARTICLE NO. CA971496

Photocatalytic Oxidation of Cyanides in Aqueous Titanium Dioxide Suspensions

Vincenzo Augugliaro,*[,1] Vittorio Loddo,* Giuseppe Marcì,* Leonardo Palmisano,* and María José López-Muñoz†

*Dipartimento di Ingegneria Chimica dei Processi e dei Materiali, Università di Palermo, Viale delle Scienze, 90128 Palermo, Italy; †Instituto de Catálisis y Petroleoquímica, C.S.I.C., Campus de la Universidad Autónoma, Cantoblanco, 28049 Madrid, Spain

Received May 15, 1996; revised October 15, 1996; accepted October 15, 1996

The photocatalytic oxidation of free cyanides in aqueous suspensions containing polycrystalline TiO_2 (anatase) powders irradiated in the near-UV region has been investigated. The rate of cyanide photooxidation has been studied by varying the following operative parameters: (i) initial cyanide concentration; (ii) catalyst concentration; (iii) initial pH; (iv) power of irradiation; and (v) chloride ion concentration in the reacting mixture. Under the used experimental conditions the photoreaction proceeded at a measurable rate until the complete disappearance of cyanides. The kinetics of cyanide photooxidation is affected by the catalyst concentration, the chloride ion concentration, and the power of irradiation while it is independent of the initial cyanide concentration and the pH. The detrimental effect of chloride ions on cyanide photooxidation rate is not determined by a competition mechanism of chloride ions with cyanide ions or oxygen molecules for adsorption on active sites. Chloride ions affect the photoreaction rate by lowering the concentration of dissolved oxygen to values for which oxygen may become a rate limiting reactant. The Langmuir–Hinshelwood kinetic model well fits all the photoreactivity results. The reaction pathway was also investigated; cyanate, nitrate, and carbonate were found to be the main oxidation products. A mass balance on nitrogen was also successfully carried out. Specific experiments were carried out in a particular setup for measuring both the photon flow absorbed by the reacting suspension and the cyanide photoreaction rate; for these particular conditions the quantum yield value was calculated.

INTRODUCTION

The presence of free and complex cyanides in industrial aqueous wastes is a problem of major concern owing to the well-known toxicity of these species for the living organisms even at very low concentration values. The conventional processes used up to-date to treat waters polluted with cyanides are mainly chemical (1) and biological (2). The alkaline chlorination process is the current technique for treating cyanide wastes; this technique shows, however, the following main limitations: (i) a highly toxic cyanogen chloride gas can be formed and released during the treatment process; and (ii) only free cyanide species are oxidised into nitrogen and carbon dioxide leaving behind the complex metal cyanides.

A promising method for treating aqueous wastes contaminated with cyanides is the photocatalytic one; this method has been found to be effective to photooxidise cyanides (3–18) dissolved in water to less dangerous species in the presence of polycrystalline semiconductor oxides under near-UV radiation. Beyond to establish the feasibility of cyanide photooxidation, the investigations have been devoted to study the use of powdered semiconductors, such as TiO_2 (3–11), platinized TiO_2 (6, 12), CdS (5, 11), ZnO (4, 8, 11, 13), WO_3 (4), or Fe_2O_3 (4), and the photoreaction mechanism. The use of visible light irradiation for the conversion of CN^- to SCN^- in the presence of Rh-loaded CdS dispersed in alkaline aqueous sulphide medium has been also reported (9). Different reaction products have been reported to be formed by using different photocatalysts. For ZnO (8) the presence of CO_3^{2-} has been found along with CNO^- while, in the presence of TiO_2 (9, 11), the main oxidation products are reported to be CNO^- and NO_3^-. Owing to the fact that the amounts of cyanides and products present in the reaction ambient did not satisfy the mass balance with respect to the initial amount of cyanide, the formation of volatile species, such as NH_3 (15), or the volatilisation of part of cyanides as HCN during the photoreaction (9, 11) has been also hypothesised. Although the to-date literature reports the occurrence of cyanides photooxidation in various experimental conditions, additional studies are required in order to fully understand the kinetic and mechanistic aspects of this photoreaction and to prove that this method can be proposed for an industrial application.

This paper is devoted to study the photocatalytic oxidation of cyanides by using a "home prepared" TiO_2 (anatase) polycrystalline catalyst. The kinetics of the photooxidation reaction has been investigated in a batch reactor by varying the following operative parameters: (i) initial cyanide

[1] Author to whom correspondence should be addressed.

0021-9517/97 $25.00

concentration; (ii) catalyst concentration; (iii) initial pH; (iv) power of irradiation; and (v) chloride ion concentration. A detailed investigation of stable intermediate products was also carried out in order to hypothesise a likely reaction mechanism. By using a method reported in the literature (19–21), the photon flow absorbed by the suspension in a particular setup under specific irradiating conditions was measured, together with the corresponding cyanide photooxidation rate. The quantum yield value of cyanide photooxidation reaction at the used experimental conditions was calculated as the ratio between the reaction rate and the photon absorption rate.

EXPERIMENTAL

Photoreactivity

The photoreactivity experiments were performed in a Pyrex batch photoreactor of cylindrical shape containing 1.5 L of aqueous suspension of polycrystalline TiO_2. Medium pressure Hg lamps (Helios Italquartz) of different electric power were immersed within the photoreactor; they were cooled by water circulating through a Pyrex jacket surrounding them. The Pyrex thimble, together with the water circulation, avoided lamp overheating and cut off any radiation with wavelength below 300 nm. The photoreactor was provided with ports in its upper section for the passage of gases, for sampling and for pH and temperature measurements. A magnetic stirrer guaranteed a satisfactory suspension of the powder and the uniformity of the reacting mixture. For all the runs the temperature of the suspension was 303 ± 2 K.

A "home prepared" TiO_2 was used for the experiments. Titanium hydroxide was precipitated by reacting an aqueous solution of $TiCl_3$ (15 wt%) with an aqueous ammonia solution (25 wt%). After repeated operations of filtration and washing with bidistilled water the resulting solid precursor was dried in air at 393 K for 24 h and subsequently heated at 773 K for 48 h. The details of the preparation method have been previously reported (22). X-ray analysis revealed that the sample obtained after the above-described thermal treatment mainly consisted of anatase. The catalyst, whose BET surface area was 57 $m^2 \cdot g^{-1}$, was classified by sieving and the fraction with particle size in the 44–125 μm range was used.

All the reagents were Carlo Erba (RPE). The quantitative determination of cyanide was routinely performed by a ion sensitive cyanide electrode (ORION mod. 94-06) in an expandable ion analyser (ORION EA 920); a standard colorimetric method (23) was also used to calibrate and periodically check the cyanide electrode.

The experimental runs were carried out always by the following procedure. The reacting mixture was prepared by suspending the desired amounts of catalyst in distilled water followed by NaOH addition in order to reach an alkaline pH; then a certain amount of KCN was added. The resulting suspension was saturated by bubbling oxygen or air at atmospheric pressure for 30 min before starting the irradiation. For a run a N_2–O_2 mixture with oxygen molar fraction of 0.1 was also used. During the run the gas was continuously bubbled so that the steady state concentration of oxygen dissolved in the solution was dependent on the composition of the bubbled gas and the ionic strength of the solution. The concentration of dissolved oxygen did not change during the runs; it was measured by using an electrode (ORION mod. 97-08) in an expandable ion analyser (ORION EA 920). Owing to the fact that steady state conditions of irradiation are achieved after about 10 min after ignition, the lamp of the photoreactor was turned on in the absence of the suspension. After 15 min from the ignition the suspension was rapidly transferred inside the photoreactor and that time was considered the zero time of the run. The majority of the runs lasted 2 h; this period of time was increased up to 6 h for the runs devoted to investigate the mechanistic aspects of cyanide photooxidation. Samples for analyses were withdrawn at fixed intervals of time and filtered through 0.45 μm cellulose acetate membrane (HA, Millipore) in order to separate the catalyst.

The influence on the cyanide photoreactivity of the following parameters was investigated: (a) initial cyanide concentration (0.192–4.04 mM); (b) initial pH (9.9, 11.6, 12.8, and 13.9); (c) catalyst concentration (0.1–3 $g \cdot L^{-1}$); (d) lamp power (500, 750, and 1000 W); and (e) NaCl concentration (0–1.41 M). It is worth noticing that K_a of hydrogen cyanide is equal to 4.9×10^{-10} at the temperature of 298 K; it is therefore necessary to work in strong alkaline conditions in order to avoid the formation of volatile HCN in the solution.

Some selected experiments were performed with the aim of determining the chemical nature of stable intermediates and final products of cyanide photooxidation. For these runs two initial pH's were used: 9.5 and 12, while the initial cyanide concentrations were 0.4 and 0.35 mM, respectively. These experiments showed that cyanate, nitrate, and carbonate were the main cyanide photooxidation products. The analyses of cyanates and nitrates were carried out by using an ionic chromatograph system (Alltech) equipped with a 350 conductivity detector and a 335 suppressor module. The columns used were Universal anion 300 (150 mm long $\times$ 4.6 mm i.d.) and Conventional anion/R (250 mm long $\times$ 4.1 mm i.d.) and were maintained at 303 K by using a 330 column heater. Aqueous solutions of $NaHCO_3$ (2.8 mM) and Na_2CO_3 (2.2 mM) were used as eluents at the flow rate of 1.83×10^{-2} $cm^3 \cdot s^{-1}$. For the determination of carbonate ions the eluent was an aqueous solution of 4-hydroxybenzoic acid to which LiOH was added until a pH value of 8.5 was reached.

In order to test the photocatalytic nature of cyanate oxidation, a few reactivity runs were carried out by using cyanate as initial reactant at the same experimental

conditions and with the same run procedure used for cyanide photooxidation.

It was also checked if ammonia was one of the photoreaction products; the ammonia determination was performed by bubbling the gas at the outlet of the photoreactor into a H_2SO_4 (1 N) aqueous solution; at the end of the run the solution was alkalinised and the ammonia was quantitatively analysed by an ion-selective electrode (ORION mod. 95-12).

Absorbed Photon Flow Determination

The experimental apparatus for photon flow determination was made of two cylindrical vessels (i.d. = 5.8 cm) of Pyrex glass, vertically positioned one on the top of the other. The upper vessel contained the aqueous suspension of the solids under investigation and an appropriate ferrioxalate actinometer solution (24) was placed in the lower one. The external surfaces of both vessels were covered by mirror-polished aluminium sheets and a Pyrex sheet was placed on the top of the upper vessel. The whole apparatus was kept inside a box of black internal walls in which an oxygen atmosphere was maintained.

The suspension was directly irradiated from the circular top surface of the upper vessel. The arc lamp supply (Oriel, 8530) was furnished by a 1000 W lamp (Hanovia, L 5173) and by a system of collimating lenses. The distance between the lenses and the top of the suspension was 52 cm and the photon flow impinging on the suspension was $\Phi_i = 5.66 \times 10^{-7}$ Einstein $\cdot s^{-1}$. The rates of backward reflected photons, Φ_r, and of absorbed photons, Φ_a, were determined according to a previously reported method (19–21) which essentially consists in measuring the transmitted photon flow, Φ_t, as a function of the suspension volume. Different volumes of aqueous suspension were used; the corresponding suspension heights were: 1.14, 1.51, 1.89, 2.27, 2.65, and 2.84 cm. The irradiation of the suspension lasted 30 s; these runs were carried out at 303 K by using always a powder concentration of 1 g $\cdot L^{-1}$ in the presence of a cyanide concentration of 0.378 mM. The pH of the suspension was adjusted to 13 by adding NaOH. During the runs the suspension and the actinometer solution were agitated by means of a magnetic stirrer. At the end of each run the absorbance of the actinometer solution was measured at the wavelength of 510 nm.

In order to determine the quantum yield value, the experimental apparatus used for photon flow determination was also utilised for carrying out a cyanide photooxidation run with a suspension height of 3.78 cm at the same experimental conditions used for the determination of the absorbed photon flow. This run lasted 80 min.

RESULTS

No oxidation of cyanides and/or cyanates was observed in the absence of light and/or of catalyst and/or of oxygen. It was also checked that the bubbling of gas into the reacting mixture did not produce a decrease of cyanide concentration due to a (unlikely) stripping effect. For all the runs, except those devoted to investigating the influence of chloride ion concentration on cyanide photooxidation, it was found that the oxygen was not a limiting reactant as the reactivity results obtained by bubbling pure oxygen or air did not show appreciable differences. This was not the case when the ionic strength of solution was greatly increased or when an O_2-poor gaseous mixture was bubbled in the solution.

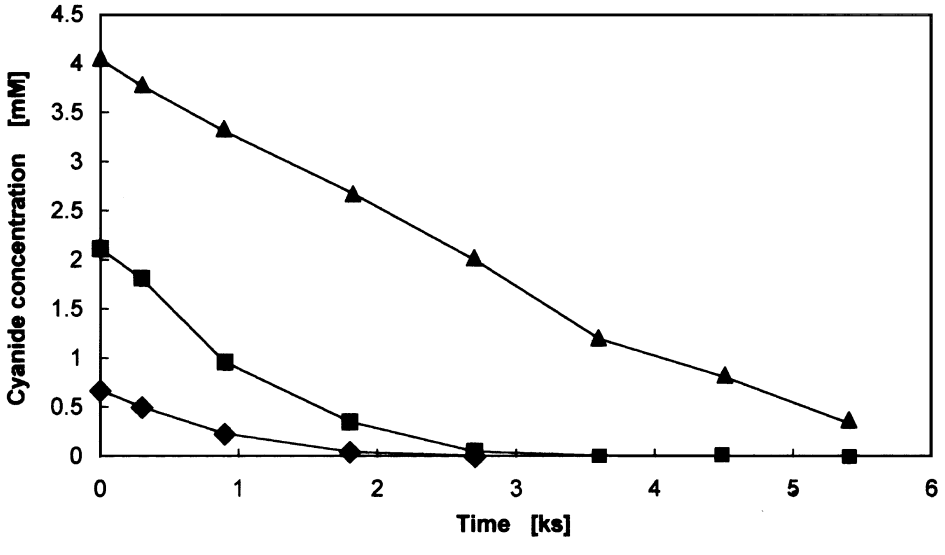

FIG. 1. Cyanide concentration versus irradiation time for runs performed at different initial cyanide concentrations. TiO_2 concentration, 3 g $\cdot L^{-1}$; pH, 12.8; lamp power, 500 W.

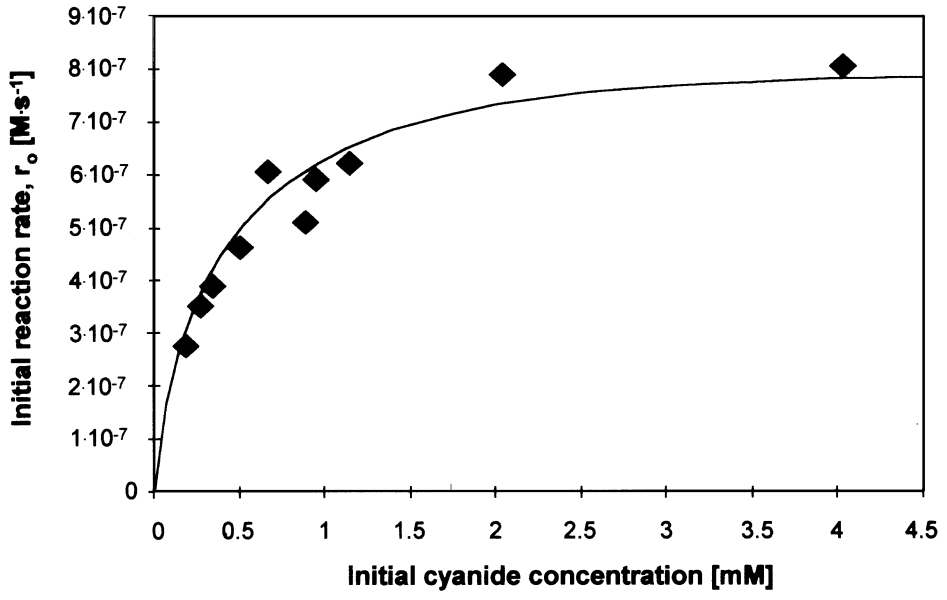

FIG. 2. Initial reaction rate of cyanide photooxidation, r_0, versus initial cyanide concentration, $c_{1,0}$. TiO_2 concentration, 3 g · L^{-1}; pH, 12.8; lamp power, 500 W.

For typical runs Fig. 1 reports on a linear scale the measured values of cyanide concentration, c_1, plotted against irradiation time, t. In Fig. 2 all the reactivity results obtained at equal reaction conditions but by varying the initial cyanide concentration, $c_{1,0}$, are reported in a linear plot as initial reaction rate, r_0, versus $c_{1,0}$.

The analyses performed on the reacting system showed that the intermediate and stable species produced during cyanide photooxidation were the following ones: cyanate, nitrate, and carbonate. In Figs. 3 and 4 the experimental results of CN^-, CNO^-, and NO_3^- concentration are reported as a function of the reaction time for experiments carried out at an initial pH of 9.5 and 12, respectively. These figures also report the nitrogen molar balance, i.e., the sum of cyanide, cyanate, and nitrate moles. The carbonate concentration values are not reported in these figures as the carbonate quantitative determination by ionic chromatography was quite difficult and the obtained figures were greatly scattered and not reliable for a total carbon molar balance.

It can be noticed from the observation of the data reported in Figs. 3 and 4 that the oxidation of CNO^- starts to be significant only after the almost complete disappearance

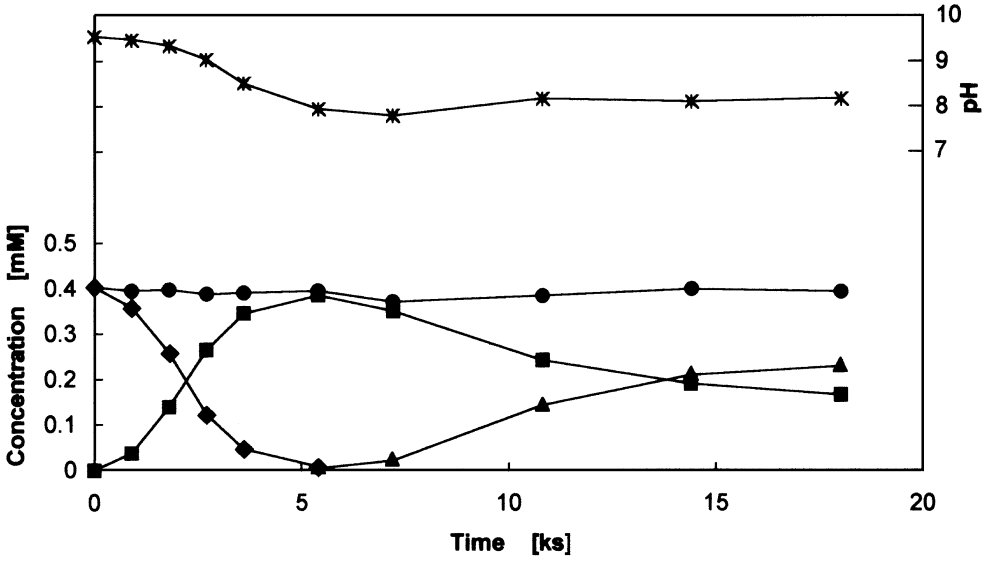

FIG. 3. Concentration of cyanide and intermediate products and pH versus irradiation time. TiO_2 concentration, 0.15 g · L^{-1}; initial pH, 9.54; lamp power, 500 W: ◆, cyanide; ■, cyanate; ▲, nitrate; ●, nitrogen molar balance; ∗, pH.

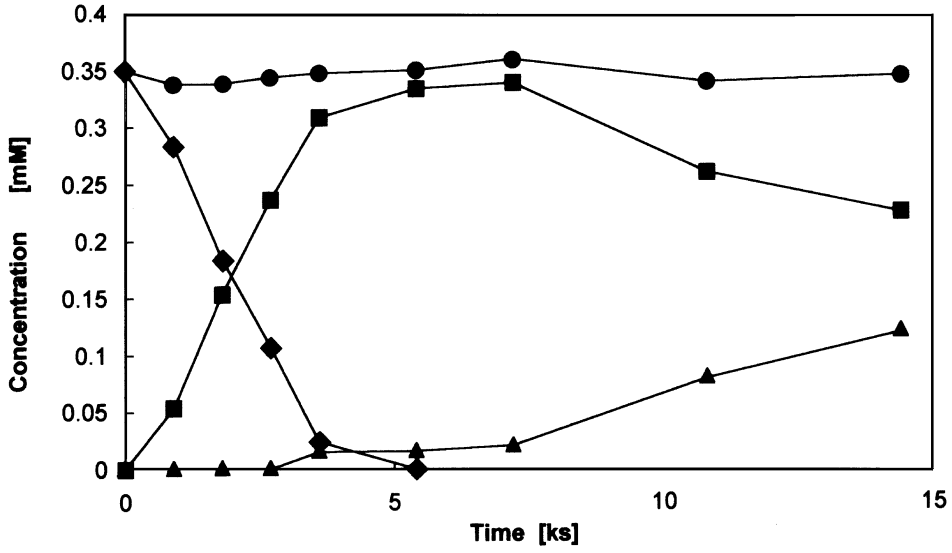

FIG. 4. Concentration of cyanide and intermediate products versus irradiation time. TiO_2 concentration, 0.15 $g \cdot L^{-1}$; initial pH, 12; lamp power, 500 W. Symbols as in Fig. 3.

of CN^- ions. NO_3^- ions appear when the CN^- concentration reaches a negligible value. The nitrates concentration increases with the reaction time; the qualitative indication given by carbonate analysis is the same: carbonate ions concentration substantially increases only when cyanide concentration reaches very low values. The measured values of cyanide, cyanate, and nitrate concentration quite well satisfy the nitrogen molar balance.

The variation of pH versus irradiation time is also reported in Fig. 3. It can be observed a continuous decrease of pH during the CN^- oxidation to CNO^- while its value remains almost constant during the subsequent photooxidation process affording carbonate and nitrate species. For the run whose results are reported in Fig. 4 the pH variation with time is not reported as it was negligible.

Figure 5 reports on a semilogarithmic plot the measured values of cyanate concentration plotted against irradiation time for runs carried out at the pH's of 8.5 and 12. In this figure the cyanide photodegradation results, obtained in runs carried out at equal reaction conditions of those of

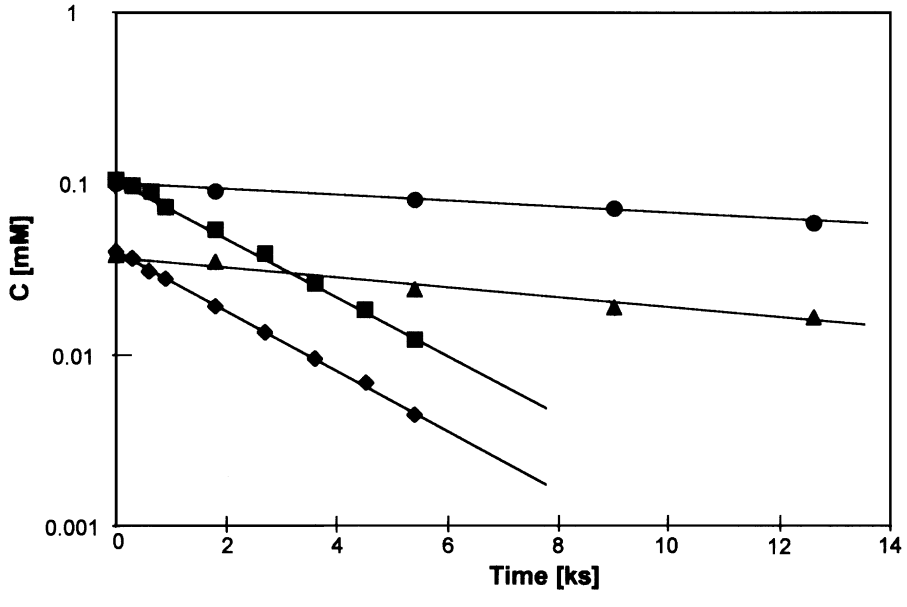

FIG. 5. Cyanide and cyanate concentrations versus irradiation time for runs performed at different initial concentrations and pH. TiO_2 concentration, 0.15 $g \cdot L^{-1}$; lamp power, 500 W: cyanide: ◆, pH = 9.5; ■, pH = 12; cyanate: ▲, pH = 8.5; ●, pH = 12.

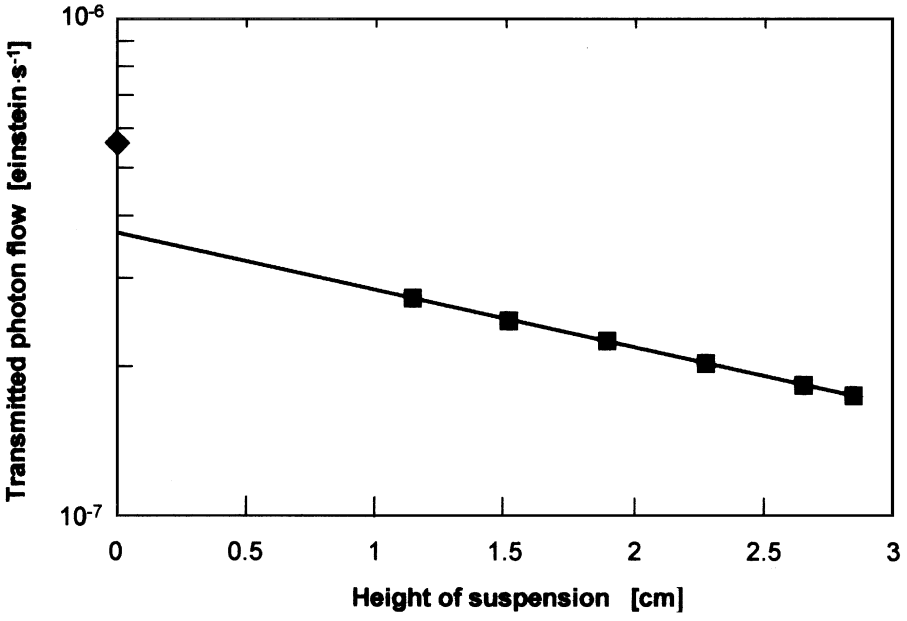

FIG. 6. Experimental results of transmitted photon flow, Φ_t versus the height of suspension, h, in the photoreactor. The (◆) symbol indicates the incident photon flow, Φ_i.

cyanate oxidation, are also reported. It may be noted that the rate of cyanate degradation is always smaller than that of cyanide and that the increase of pH negatively affects the cyanate oxidation rate.

The experimental results of actinometer runs are reported in the semilogarithmic plot of Fig. 6 as transmitted photon flow, Φ_t, versus the height, h, of suspension contained in the photoreactor. The value of the incident photon flow, Φ_i, is also reported in this figure.

DISCUSSION

Mechanistic Aspects

In a photocatalytic process the primary step following the radiation absorption by the photocatalyst is the generation of electron–hole pairs which must be trapped in order to avoid recombination (charge separation):

$$TiO_2 + h\nu \rightarrow TiO_2 + e^-_{CB} + h^+_{VB}. \quad [1]$$

The hydroxyl groups are the likely traps for holes,

$$TiO_{2(substrate)}\text{–}OH^-_s + h^+ \rightarrow TiO_{2(substrate)}\text{–}OH\cdot_{(ads)}, \quad [2]$$

leading to the formation of hydroxyl radicals which are strong oxidant agents. The traps for electrons are adsorbed oxygen species according to the following equations:

$$O_{2(aqueous\ solution)} \rightleftarrows O_{2(ads)} \quad [3]$$

$$O_{2(ads)} + e^- \rightarrow O^-_{2(ads)}. \quad [4]$$

The superoxide species are unstable and reactive and they may evolve in several ways. It is useful to stress the point that in a photoreaction occurring on a semiconductor catalyst powder both the oxidation and reduction processes must occur on the same particle, although reaction sites for these processes may be different (25). In conclusion, as a consequence of the primary step of electrons and holes trapping, several species are produced which will be involved in the reaction mechanism.

It has been shown in several studies (4, 7, 9, 11) that CNO^- is the first product in the photocatalytic oxidation of cyanides in the presence of polycrystalline TiO_2 in aqueous medium. The mechanism proposed by Frank and Bard (4) implies the oxidation of the inorganic species by the photogenerated holes in the semiconductor and the reduction of oxygen by the conduction band electrons according to the following reactions:

$$CN^- + 2OH^- + 2h^+ \rightarrow CNO^- + H_2O, \quad [5]$$

$$O_2 + 2e^- + 2H_2O \rightarrow H_2O_2 + 2OH^-, \quad [6]$$

or

$$\tfrac{1}{2}O_2 + 2e^- + H_2O \rightarrow 2OH^-. \quad [7]$$

According to other studies, however, cyanate ion has not been found to be the final oxidation product. Indeed, Peral *et al.* (7) report the subsequent formation of CO_3^{2-} and N_2 while Pollema *et al.* (9) and Mihaylov *et al.* (11) detect the formation of CO_2, NO_2^- and NO_3^-. In all of the above studies a lack of mass balance between cyanide and final products was found and several explanations,

hypothesising the formation of volatile species, have been reported.

The results obtained in the present work confirm that CNO^- is the first product in the photooxidation process. The observed absence of NO_2^- and of NH_3 among the reaction products, probably due to strong oxidant conditions used in all the experiments, indicates that CNO^- is subsequently oxidised to CO_2 and NO_3^- ions according to the following reaction:

$$CNO^- + 8OH^- + 8h^+ \rightarrow NO_3^- + CO_2 + 4H_2O. \quad [8]$$

By properly combining Eqs. (8) and (6), the overall reaction for CNO^- photooxidation can be expressed as

$$CNO^- + 4O_2 + 4H_2O \rightarrow NO_3^- + CO_2 + 4H_2O_2. \quad [9]$$

From the results reported in Figs. 3 and 4 it is worth noticing, moreover, that CNO^- photooxidation rate depends on the initial pH while the photooxidation rate of CN^- is not significantly affected by this parameter. The results of the runs performed with CNO^- as initial reactive species at 8.5 and 12 pH's (see Fig. 5) indicate a decrease of the CNO^- degradation rate by increasing the pH, as reported by Bravo *et al.* (26). From the above considerations it can be hypothesised that Frank and Bard (3) did not observe a further oxidation of CNO^- due to its very low degradation rate at high pH values.

As to concern the variation pattern of pH during the photoprocess, an explanation of the pH decrease during the CN^- oxidation to CNO^- can be given taking into account the different basic strengths of CN^- and CNO^- in the first stage of the photoprocess ($pK_{a,HCN} = 9.3$; $pK_{a,HCNO} = 3.9$ at $T = 298$ K). It may be noticed that the reactions [5] and [6] do not imply any variation of hydroxyl ion concentration. On the other hand, when cyanide completely disappears and cyanate and nitrate appear, the buffer effect due to the production of carbon dioxide could be responsible of the substantially constancy of the pH value (see reaction [9]). Indeed in the alkaline pH range at which the photoreaction has been investigated carbon dioxide exists as carbonate and/or hydrogen carbonate ions whose relative amounts strongly depend on the pH.

Kinetic Aspects

From the reactivity data reported in Fig. 1, it may be noticed that a straight line fits the data at high values of cyanide concentration while at low values an exponential line seems to better fit the data. This pattern was shown by all the experimental runs. From the data reported in Figs. 3 and 4 it may be noticed that cyanate photooxidation significantly starts only when the cyanide ions almost disappear; the rate of cyanate photooxidation is quite smaller than that of cyanide. On this basis it may be assumed that: (a) the cyanide photooxidation reaction proceeds according to zero order kinetics at high concentration of cyanide; (b) the reaction turns to pseudo-first-order kinetics when the cyanide concentration decreases; and (c) the cyanate photocatalytic oxidation only starts after the (almost) complete oxidation of cyanide ions. This last assumption implies that the competition for adsorption on the same sites between cyanide and cyanate ions is significantly in favour of cyanide ions; the validity of this assumption and the negligible approximation introduced by it in the kinetic model are discussed by Augugliaro *et al.* (27). On this ground a chemical kinetic model able to explain the experimental indications is here proposed.

The rate determining step of the photooxidation process is hypothesised to be the reaction between $OH\cdot$ radicals and cyanide ion over the catalyst surface. As the adsorbed oxygen acts as an electron trap thus hindering the electron–hole recombination, the $OH\cdot$ radicals concentration depends on the fractional sites coverage by O_2. Two different types of sites are hypothesised to exist on the catalyst surface. The first ones are able to adsorb cyanide ions while the second ones are able to adsorb oxygen. In this hypothesis the reaction rate for second-order surface oxidation of cyanide may be written in terms of Langmuir–Hinshelwood kinetics as

$$r = k'' \cdot \theta_{oxygen} \cdot \theta_{cyanide} \quad [10]$$

in which k'' is the surface second-order rate constant, and θ_{oxygen} and $\theta_{cyanide}$ are the fractional sites coverages by oxygen and cyanide, respectively.

The fractional sites coverages by cyanide ions and by oxygen are given by

$$\theta_{cyanide} = \frac{K_1 c_1}{1 + K_1 c_1} \quad [11]$$

$$\theta_{oxygen} = \frac{K_2 c_2}{1 + K_2 c_2} \quad [12]$$

in which K_1 and K_2 are the equilibrium adsorption constants of cyanide and oxygen, respectively, and c_1, and c_2, the cyanide and oxygen concentrations in the aqueous phase. Owing to the fact that all the experiments were performed in a batch reactor by continuously bubbling oxygen to the liquid phase, it may be assumed that for all the runs the θ_{oxygen} term is constant during the occurrence of cyanide photooxidation. Equation [10] can therefore be written as

$$r = k' \cdot \theta_{cyanide} \quad [13]$$

in which k' is the surface pseudo-first-order rate constant and it is equal to $k'' \cdot \theta_{oxygen}$. The k' values obviously depend on the θ_{oxygen} ones so that caution must be used in comparing k' values obtained in different runs. For runs performed at equal concentration of dissolved oxygen, the k' values can be correctly compared among them. The comparison of runs performed with different concentrations of dissolved

oxygen is also correct when the reactivity becomes independent of the oxygen concentration. By substituting Eq. [11] into Eq. [13], the following differential equation is obtained:

$$r = -\frac{dc_1}{dt} = \frac{k' K_1 c_1}{1 + K_1 c_1}. \qquad [14]$$

Equation [14] can be easily integrated with the limiting condition that at the start of the reaction, $t = 0$, the cyanide ion concentration is the initial one, $c_1 = c_{1,0}$; the integral relationship between c_1 and t is therefore

$$t = A \ln\left(\frac{c_{1,0}}{c_1}\right) + B(c_{1,0} - c_1) \qquad [15]$$

in which

$$A = 1/k' K_1 \qquad [16]$$

and

$$B = 1/k'. \qquad [17]$$

By applying a least-square best fitting procedure to the photoreactivity experimental data, for each run the values of A and B have been determined; from the mean values of A and B the following values of $K_1 = 2.7 \times 10^3\ \mathrm{M}^{-1}$ and $k' = 8.2 \times 10^{-7}\ \mathrm{M \cdot s}^{-1}$ have been calculated. By substituting the K_1 and k' values into Eq. [14], the analytical relationship between r_0 and $c_{1,0}$ is obtained. The continuous line drawn in Fig. 2 represents this relationship; a good fitting of the model to the experimental data may be observed thus confirming the Langmuir–Hinshelwood nature of the photoreaction mechanism.

As previously reported, the runs performed without the addition of NaCl to the solution exhibited reactivity results with negligible differences depending on the nature of the bubbling gas (pure oxygen or air). There are two possible ways of explaining this finding. The first one is that a θ_{oxygen} values of unity is achieved. The second possibility is that the oxygen partial pressure above which the reaction rate does not further increase is related to the existence of a critical value of oxygen concentration for which all photoelectrons arriving to the surface are captured. On the basis only of the reactivity results here presented, it is not possible to indicate which of the two possibilities is the correct one; however, the validity of the kinetic model is not affected at all, whatever the real process is.

From the cyanate photoreactivity results reported in Fig. 5, it may be noticed that the cyanate degradation process exhibits a pseudo-first-order kinetics with respect to cyanate concentration, c_{cyanate}, whose integrated equation is

$$c_{\mathrm{cyanate}} = c^{\circ}_{\mathrm{cyanate}} \exp(-k_{\mathrm{cyanate}} \cdot t) \qquad [18]$$

in which k_{cyanate} is the pseudo-first-order rate constant and $c^{\circ}_{\mathrm{cyanate}}$ the initial cyanate concentration. By applying a least-square best fitting procedure to the c_{cyanate}-t data reported in Fig. 5, the values of k_{cyanate} at the pH's of 8.5 and 12 were obtained; they are 7.5×10^{-5} and $4 \times 10^{-5}\ \mathrm{s}^{-1}$, respectively.

Figure 7 reports in a linear diagram the values of k' versus the catalyst concentration, c_{cat}. The values of k' increase by increasing the catalyst concentration, reach a maximum at about $c_{\mathrm{cat}} = 2\mathrm{g \cdot L}^{-1}$ and therefore they smoothly decrease. This dependence of the kinetic constant on the catalyst concentration is reported in the literature (28). It must be noticed that, in contrast to heterogeneous catalysis, the increase of the catalyst concentration has two opposite

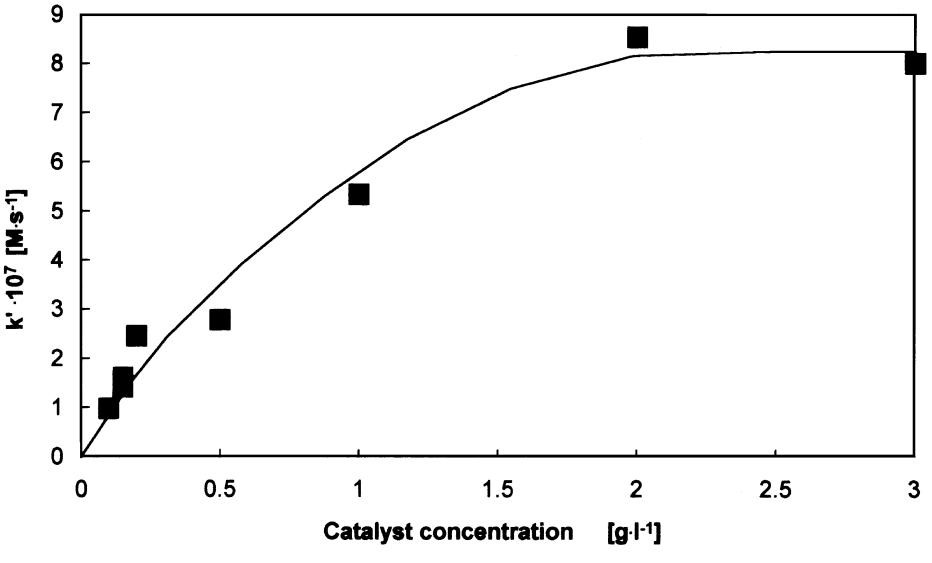

FIG. 7. Values of the surface pseudo-first-order rate constant, k', versus the catalyst concentration. Initial cyanide concentration, 0.338–0.385 mM; pH, 12.9–13.9; lamp power, 500 W.

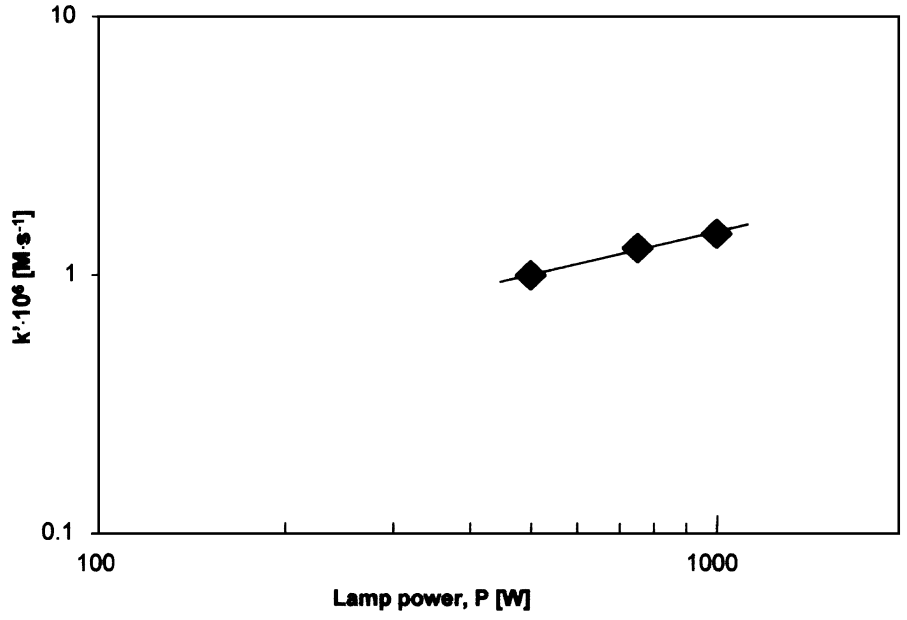

FIG. 8. Values of the surface pseudo-first-order rate constant, k', versus the lamp power, P. Initial cyanide concentration, 2.07 mM; pH, 12.9; catalyst concentration, 3 g · L^{-1}.

effects on the photoreactivity. The beneficial effect is that the whole surface is exposed to the radiation, and therefore, the total number of active sites increases. The detrimental effect is that the local radiation intensity, which is one of the driving forces of the photoprocess, decreases by increasing the catalyst concentration. As long as the catalyst concentration increase determines an increase of the total photons absorbed by the whole reacting system, the kinetic constant k' increases but, when the photons transmitted by the suspension become negligible, the reactivity increase stops. The decrease of the kinetic constant after the maximum can be justified by considering that the increase of TiO_2 concentration determines a major shielding effect from the radiation source for the farthest catalyst particles.

Figure 8 reports in a logarithmic diagram the values of k' against the lamp power, P. The values of k' increase by increasing P thus indicating, as it is well known (29), that the lamp power has a beneficial effect on the photoreactivity. The cyanide adsorption constants, K_1, were quite insensitive to the lamp power, as expected; their values for 500, 750, and 1000 W lamp powers were 2.7×10^3, 2.9×10^3, and 2.9×10^3 M^{-1}, respectively. A power law relationship of the form: $k' \cap P^{\alpha}$ has been best fitted through the data; the straight line drawn among the data in Fig. 8 corresponds to a value of α of 0.57. For heterogeneous photocatalytic reactions occurring at high radiation intensity a square-root dependence of the kinetic constant on the light intensity has been reported (29, 30). A likely explanation of this behaviour is that at increasing *e-h* generation rate (determined by the high radiation intensities) there is the predominance of the rate of *e-h* recombination with respect to the rate of *e-h* capture by species involved in the chemical reaction.

From the runs for which only the initial pH was varied the values of k' and K_1, calculated as reported before, do not show appreciable dependence on this parameter. It may be therefore concluded that cyanide photoreactivity and photoadsorption on TiO_2 surface are independent of the pH, at least in the 9.9–13.9 range investigated in the present work.

The pertinent literature reports a detrimental effect of chloride ions on the photodegradation rate of organic molecules. Boonstra and Mutsaers (31) report that the presence of chloride ions in the solution decreases the oxygen photoadsorption as chloride ions decrease the hydroxyl groups content of TiO_2 powders. Abdullah *et al.* (32), by investigating the effects of common inorganic anions on rates of photocatalytic oxidation of organic molecules over irradiated TiO_2, report a decrease of the rate of oxidation by increasing the chloride concentration. The detrimental effect of chloride ions is explained by a model in which the adsorbed anions compete with adsorbed organic species for oxidising sites on the TiO_2 surface to give oxidising inorganic radical anions. If one or both of the previous inhibitory mechanisms would be effective for cyanide photooxidation, the photoreactivity should continuously decrease by increasing the chloride concentration; i.e., the photoreactivities in the absence and in the presence of chloride ions should be always different.

For the reactivity runs performed with the aim of investigating the influence of chloride ions on the cyanide

TABLE 1

Main Operative Parameters, Together with the Calculated Values of the Pseudo-First-Order Rate Constant, k', for Runs Carried Out with the Aim of Investigating the Influence of Chloride Ions on Cyanide Photodegradation Rate

Initial cyanide concentration mM	pH	Bubbling gas	Chloride ions concentration M	Dissolved oxygen concentration mM	$k' \times 10^7$ $M \cdot s^{-1}$
0.96	12.3	Pure oxygen	0	1.063	8.54
0.93	12.1	Pure oxygen	1.41	0.688	8.64
0.93	12.2	Air	0	0.206	8.44
0.85	11.9	Air	1.41	0.138	5.45
1	12.0	Oxygen-poor O_2–N_2 mixture	0	0.094	3.18
0.88	12.2	Oxygen-poor O_2–N_2 mixture	1.41	0.063	2.28

Note: TiO_2 concentration: 3 $g \cdot L^{-1}$; lamp power, 500 W.

photodegradation rate, Table 1 reports the values of the main operative parameters of the runs, together with the values of k' obtained by the best fitting procedure applied to the experimental data. This table also reports the measured values of dissolved oxygen concentration, c_2. It may be noticed that the values of k' are not related to the chloride concentration but to the oxygen concentration. In Fig. 9 the values of k' are reported in a linear plot as a function of c_2. The results indicate an increase in k' up to an oxygen concentration of about 0.2 mM; at higher concentrations the k' values are constant. The pattern of the data reported in this figure clearly indicates that a Langmuir adsorption kinetics of oxygen on the TiO_2 surface is the rate determining step for an oxygen concentration value smaller than 0.2 mM. Beyond this value oxygen is not a limiting reactant so that the process rate becomes insensitive to the variations of oxygen concentration; this last feature also indicates the absence of O_2-related mass transfer resistances on the cyanide photooxidation rate.

It is well known that the solubilities of gases in water change with the composition of the aqueous solution, being dependent on the ionic strength of the solution and the chemical nature of the anions and cations involved. This effect is sometimes referred to as the "salting out" effect (33). In the presence of strong electrolytes, such as NaCl, the solubility of oxygen is lower than in pure water. For the photocatalytic process here investigated the addition of ions to the solution eventually decreases the concentration of dissolved oxygen but the rate of the photoreaction does not decrease if the oxygen is not a limiting reactant. The rate of cyanide photodegradation starts to decrease only when the saline composition of the solution determines a critical value of oxygen concentration. As previously discussed, this oxygen concentration value can be that for which θ_{oxygen} is unity or that for which the resulting θ_{oxygen} is able to capture all the produced photoelectrons. In conclusion the observed decrease of the cyanide photoreactivity is not linked to the specific nature of the electrolyte but to the fact that the electrolyte, beyond a certain composition, lowers the dissolved oxygen concentration to a value for which it becomes a limiting reactant.

By remembering that $k' = k'' \cdot \theta_{oxygen}$ and that the relationship between θ_{oxygen} and c_2 is the Langmuir one expressed by Eq. [12], a least-square best fitting procedure applied to the $k' - c_2$ data reported in Fig. 9 gives for K_2, the oxygen adsorption constant, a value of 2.6×10^3 M^{-1}.

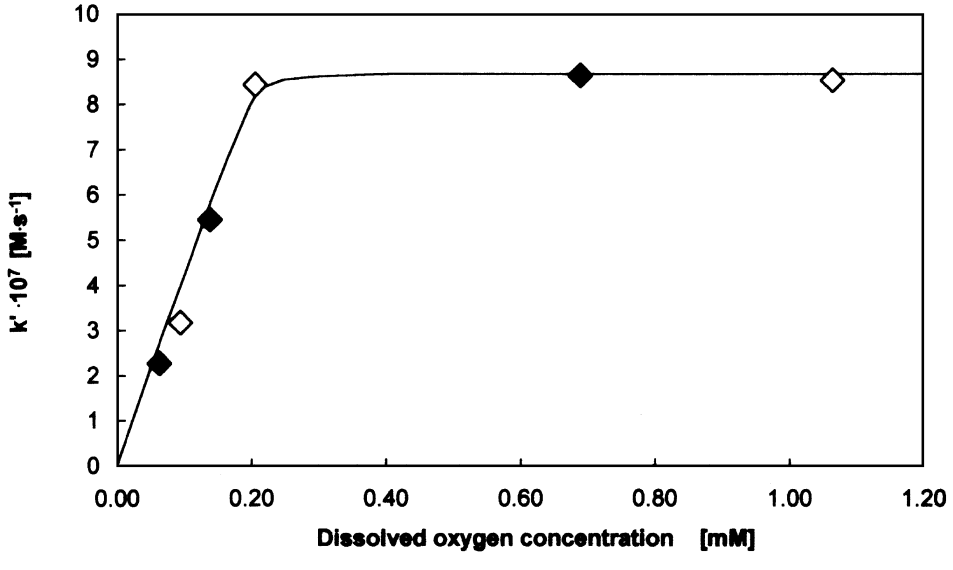

FIG. 9. Values of the surface pseudo-first-order rate constant, k', versus the oxygen concentration in the solution. TiO_2 concentration, 3 $g \cdot L^{-1}$; lamp power, 500 W. ◇ in the absence; ◆ in the presence of chloride ions.

Photophysical Aspects

From the observation of actinometer results reported in the semilogarithmic plot of Fig. 6, it may be noticed that the data lie on a straight line to a good approximation thus indicating that the following relationship, similar to the Lambert–Beer law, holds (21),

$$\Phi_t = \Phi' \cdot \exp(-E \cdot c_{\text{cat}} \cdot A \cdot h), \qquad [19]$$

in which Φ' is the rate of photons able to penetrate the suspension, E is the apparent Napierian extinctance coefficient, A is the cross section of the photoreactor, and h is the height of suspension contained in the photoreactor. The E coefficient is a characteristic optical parameter of the photocatalyst at equal particle size distribution. By applying a least-square best fitting procedure to the experimental data of Φ_t versus h, the following values of the unknown parameters of Eq. [19] have been obtained: $\Phi' = 3.76 \times 10^{-7}$ Einstein $\cdot\, s^{-1}$ and $E = 10.2\ g^{-1}$.

It may be noticed that Eq. [19] does not satisfy the condition that for $h = 0$, i.e., in the absence of photocatalyst, the Φ_t value coincides with the value of the incident photon flow, Φ_i, but it is quite smaller than Φ_i. In previous papers (19–21) the same discrepancy was observed for polycrystalline TiO_2 suspensions and it was demonstrated that this difference is proportional to the backward reflected photon flow. The difference between the incident photon flow and the value of Φ_t extrapolated at the limit condition of absence of catalyst, $\Phi_{t,h=0}$, represents the backward reflected photons, Φ_r.

By performing an integral photon balance on the photoreactor, the absorbed photon flow can be calculated by the relationship

$$\Phi_a = \Phi_i - \Phi_t - \Phi_r = \Phi_i - \Phi_t - (\Phi_i - \Phi_{t,h=0}), \qquad [20]$$

in which the last l.h.s. term only contains measurable quantities.

From the photoreactivity runs performed with the same apparatus used for determining the absorbed photon flow it was found that the cyanide photodegradation rate may be satisfactorily expressed by a zero-order kinetics whose integrated equation is

$$c_{1,0} - c_1 = k_0 t, \qquad [21]$$

in which k_0 is the zero-order rate constant. By applying a least-square best fitting procedure to the photoreactivity data the value of $k_0 = 3.1 \times 10^{-6}\ M \cdot s^{-1}$ was obtained.

The quantum yield of cyanide photodegradation, defined as the ratio between the cyanide molecules reacted per unit time and the photons absorbed per unit time was calculated in the following way. The number of cyanide molecules reacted per unit time was determined from the value of k_0 and the rate of absorbed photons was obtained by applying the integral photon balance (Eq. [20]) to a suspension with height of 3.78 cm. It is assumed that in the period of duration (30 s) of the actinometer runs, from which the absorbed photons were eventually determined, only cyanide ions are present in the reacting mixture so that the aliquot of absorbed photons useful for the photoreaction is utilised only for cyanide degradation.

The value of quantum yield of cyanide photooxidation for the above reported experimental conditions was 0.23. This value may be considered quite high; for the photooxidation of an organic molecule such as phenol the value of quantum yield, calculated in the same experimental conditions and using the same catalyst, was of about 0.1 (21).

The above reported values of quantum yield have not a general validity as the appropriate definition of quantum yield is

$$qy = \frac{\text{reaction rate}}{\text{photon absorption rate}} = \frac{\text{Const} \cdot \theta_{\text{oxygen}} \cdot \theta_{\text{cyanide}} \cdot \Phi_a^{\alpha}}{\Phi_a}. \qquad [22]$$

It is therefore evident that different values of qy can be obtained for the same photoreacting system by changing the operative conditions.

CONCLUSIONS

The photocatalytic oxidation of free cyanides has been carried out in aqueous suspensions containing polycrystalline TiO_2 (anatase) powders irradiated in the near-UV region. Under the used experimental conditions the photoreaction proceeds at a measurable rate until the complete disappearance of cyanides. The kinetic model of Langmuir–Hinshelwood well describes the photoreactivity results. The kinetics of cyanide photooxidation is affected in a positive way by the catalyst concentration and the power of irradiation and in a detrimental way by the chloride ion concentration while it is independent of the pH. The detrimental effect of chloride ions on cyanide photooxidation rate is not determined by a competition mechanism of chloride ions with cyanide ions or oxygen molecules for adsorption on active sites. Chloride ions affect the photoreaction rate by lowering the concentration of dissolved oxygen to values for which oxygen may become a rate limiting reactant. The main oxidation products of cyanide are cyanate, nitrate, and carbonate. The cyanate photocatalytic oxidation rate is smaller than that of cyanide and it obeys a pseudo-first-order kinetics with respect to cyanate concentration. The quantum yield of cyanide photooxidation reaction has been determined in a particular setup under specific conditions of reaction and irradiation; its value is quite a bit higher than that obtained for organic molecules at equal experimental conditions.

ACKNOWLEDGMENTS

The authors thank the referees for their valuable comments and suggestions. Financial support from the "Ministero dell'Università e della Ricerca

Scientifica e Tecnologica" (MURST, Rome) is gratefully acknowledged. One of the Authors (MJLM) wishes to thank the "Ministerio de Educación y Ciencia" (Madrid, Spain) for the award of a fellowship to enable part of this work to be carried out at the "Dipartimento di Ingegneria Chimica dei Processi e dei Materiali" of the University of Palermo (Italy).

REFERENCES

1. Futakawa, M., Takahashi, H., Inoue, G., and Fujioka, T., *Desal.* **98**, 345 (1994).
2. Salomonson, L. P., *in* "Cyanide in Biology" (B. Vennesland, E. E. Conn, C. J. Knowles, J. Westley, and F. Wissing, Eds.). Academic Press, New York, 1981.
3. Frank, S. N., and Bard, A. J., *J. Am. Chem. Soc.* **99**, 303 (1977).
4. Frank, S. N., and Bard, A. J., *J. Phys. Chem.* **81**, 1484 (1977).
5. Frank, S. N., and Bard, A. J., *J. Am. Chem. Soc.* **99**, 4667 (1977).
6. Rose, T. L., and Nanjundiah, C., *J. Phys. Chem.* **89**, 3766 (1985).
7. Peral, J., Muñoz, J., and Doménech, X., *J. Photochem. Photobiol. A: Chem.* **55**, 251 (1990).
8. Peral, J., and Doménech, X., *J. Chem. Tech. Biotechnol.* **53**, 93 (1992).
9. Pollema, C. H., Hendrix, J., Milosavljevic, E. B., Solujic, L., and Nelson, J. H., *J. Photochem. Photobiol. A: Chem.* **66**, 235 (1992).
10. Hidaka, H., Nakamura, T., Ishizaka, A., Tsuchiya, M., and Zhao, J., *J. Photochem. Photobiol. A: Chem.* **66**, 367 (1992).
11. Mihaylov, B. V., Hendrix, J. L., and Nelson, J. H., *J. Photochem. Photobiol. A: Chem.* **72**, 173 (1993).
12. Kogo, K., Yoneyama, H., and Tamura, H., *J. Phys. Chem.* **84**, 1705 (1980).
13. Doménech, J., and Peral, J., *Solar Energy* **41**, 55 (1988).
14. Borgarello, E., Terzian, R., Serpone, N., Pelizzetti, E., and Barbeni, M., *Inorg. Chem.* **25**, 2135 (1986).
15. Serpone, N., Borgarello, E., Barbeni, M., Pelizzetti, E., Pichat, P., Hermann, J.-M., and Fox, M. A., *J. Photochem.* **36**, 373 (1987).
16. Zhang, J., Hendrix, J. L., and Wadsforth, M. E., *in* "Proc. EPD Congress 1991" (D. R. Gaskell, Ed.), p. 665. The Minerals, Metals and Materials Society, San Diego, CA, 1991.
17. Bhakta, D., Shukla, S. S., Chandrasekharaiah, M. S., and Margrave, J. L., *Environ. Sci. Technol.* **26**, 625 (1992).
18. Ahmed, M. S., and Attia, Y. A., *J. Non-Cryst. Solids* **186**, 402 (1995).
19. Schiavello, M., Augugliaro, V., and Palmisano, L., *J. Catal.* **127**, 332 (1991).
20. Augugliaro, V., Schiavello, M., and Palmisano, L., *A.I.Ch.E. J.* **37**, 1096 (1991).
21. Augugliaro, V., Loddo, V., Palmisano, L., and Schiavello, M., *J. Catal.* **153**, 32 (1995).
22. Soria, J., Conesa, J. C., Augugliaro, V., Palmisano, L., Schiavello, M., and Sclafani, A., *J. Phys. Chem.* **95**, 274 (1991).
23. Greenberg, A. E., Clesceqi, L. S., and Eaton, A. D. (Eds.), "Standard Methods for the Examination of Water and Wastewater." Am. Public Health Assoc., Washington, DC, 1992.
24. Murov, S. L. (Ed.), "Handbook of Photochemistry." Dekker, New York, 1973.
25. Reiche, H., Dunn, W. W., and Bard, A. J., *J. Phys. Chem.* **83**, 2248 (1979).
26. Bravo, A., Garcia, J., Domènech, X., and Peral, J., *Electrochimica Acta* **39**, 2461 (1994).
27. Augugliaro, V., Loddo, V., Marcì, G., Palmisano, L., and López-Muñoz, M. J., *in* "Proc. European Meeting on Process Industry and Environment II" (N. Piccinini and R. Delorenzo, Eds.), Vol. 1 p. 147. Politecnico di Torino, Turin, 1996.
28. Augugliaro, V., Palmisano, L., Sclafani, A., Minero, C., and Pelizzetti, E., *Toxicol. Environ. Chem.* **16**, 89 (1988).
29. Egerton, T. A., and King, C. J., *J. Oil Col. Chem. Assoc.* **62**, 386 (1979).
30. Pichat, P., *in* "Photoelectrochemistry, Photocatalysis and Photoreactors. Fundamentals and Developments" (M. Schiavello, Ed.), p. 425. Reidel, Dordrecht, 1985.
31. Boonstra, A. H., and Mutsaers, C. A. H. A., *J. Phys. Chem.* **79**, 1694 (1975).
32. Abdullah, M., Low, G. K.-C., and Matthews, R. W., *J. Phys. Chem.* **94**, 6820 (1990).
33. Danckwerts, P. V., "Gas–Liquid Reactions," pp. 18–20. McGraw–Hill, New York, 1970.